

A Redox-Dependent Pathway for Regulating Class II HDACs and Cardiac Hypertrophy

Tetsuro Ago,¹ Tong Liu,² Peiyong Zhai,¹ Wei Chen,² Hong Li,² Jeffery D. Molkentin,³ Stephen F. Vatner,¹ and Junichi Sadoshima^{1,*}

¹Department of Cell Biology and Molecular Medicine, Cardiovascular Research Institute, University of Medicine and Dentistry of New Jersey, New Jersey Medical School, Newark, NJ 07103, USA

²Center for Advanced Proteomics Research and Department of Biochemistry and Molecular Biology, UMDNJ, New Jersey Medical School Cancer Center, Newark, NJ 07103, USA

³Department of Pediatrics, University of Cincinnati, Cincinnati Children's Hospital Medical Center, Cincinnati, OH 45229, USA

*Correspondence: sadoshju@umdnj.edu

DOI 10.1016/j.cell.2008.04.041

SUMMARY

Thioredoxin 1 (Trx1) facilitates the reduction of signaling molecules and transcription factors by cysteine thiol-disulfide exchange, thereby regulating cell growth and death. Here we studied the molecular mechanism by which Trx1 attenuates cardiac hypertrophy. Trx1 upregulates DnaJb5, a heat shock protein 40, and forms a multiple-protein complex with DnaJb5 and class II histone deacetylases (HDACs), master negative regulators of cardiac hypertrophy. Both Cys-274/Cys-276 in DnaJb5 and Cys-667/Cys-669 in HDAC4 are oxidized and form intramolecular disulfide bonds in response to reactive oxygen species (ROS)-generating hypertrophic stimuli, such as phenylephrine, whereas they are reduced by Trx1. Whereas reduction of Cys-274/Cys-276 in DnaJb5 is essential for interaction between DnaJb5 and HDAC4, reduction of Cys-667/Cys-669 in HDAC4 inhibits its nuclear export, independently of its phosphorylation status. Our study reveals a novel regulatory mechanism of cardiac hypertrophy through which the nucleocytoplasmic shuttling of class II HDACs is modulated by their redox modification in a Trx1-sensitive manner.

INTRODUCTION

Reduction and oxidation (redox) is an important mechanism of posttranslational modification (Berndt et al., 2007). Reactive oxygen species (ROS) produced from various sources, such as mitochondrial leakage and NAD(P)H oxidases, oxidize signaling molecules and transcription factors. Thiol groups (R-SH) of specific cysteine residues are often oxidized to sulfenic acids (R-SOH) reversibly and to sulfinic (R-SO₂⁻) or sulfonic (R-SO₃²⁻) acids irreversibly (Berndt et al., 2007). Sulfenic acids further form intra- or intermolecular disulfide bonds (R-S-S-R) or mixed disulfide bonds with glutathione (R-S-SG; glutathionylation). Disulfide bonds and glutathionylation induce a conformational change in the molecule, thereby regulating enzymatic

activity, protein-protein interaction, and subcellular localization (Berndt et al., 2007; Nakamura et al., 1997).

Cells have two kinds of system to counteract ROS. The first group of molecules eliminates excess ROS directly; superoxide dismutases convert superoxide to hydrogen peroxide (H₂O₂), and catalases and peroxidases catalyze the production of water from H₂O₂. The other group includes glutathione (Glu-Cys-Gly) and thioredoxin (Trx), which reduce thiol groups of oxidized proteins (Berndt et al., 2007). Trx1 is a 12 kD protein that regulates signaling molecules and transcription factors and mediates redox-regulated gene expression. During reduction of target proteins, Trx1 is oxidized to form a disulfide bond between the two cysteine residues at 32 and 35 in its catalytic core (Figure S1 available online). The oxidized Trx1 is then reduced and regenerated by thioredoxin reductase and NADPH. Trx1, Trx reductase, and NADPH, collectively called the Trx system, operate as a powerful protein disulfide reductase system (Berndt et al., 2007; Nakamura et al., 1997).

Redox states critically affect the function of the heart. Both oxidative and reductive stress are involved in the pathogenesis of cardiac hypertrophy and heart failure (Cave et al., 2006; Rajasekaran et al., 2007). Cardiac hypertrophy, defined by the enlargement of ventricular mass, is initially adaptive against hemodynamic overloads, such as high blood pressure. However, the long-term presence of hypertrophy often leads to heart failure, possibly because of increased cell death. ROS regulate signaling molecules and transcription factors involved in hypertrophy and cell death. At low levels (10–30 μM), H₂O₂, a cell-permeable ROS, is associated with hypertrophy, but at higher levels, it is associated with apoptosis or necrosis in cardiac myocytes (Kwon et al., 2003). ROS play an important role in mediating cardiac hypertrophy stimulated by hemodynamic overload, as well as by agonists for G protein-coupled receptors, such as phenylephrine (PE) and angiotensin II (Hirotsu et al., 2002). In contrast, ROS-eliminating molecules, such as superoxide dismutases (Siwik et al., 1999) and catalase (Li et al., 1997), play protective roles in diseased hearts. Likewise, Trx1 attenuates heart cell death after ischemia-reperfusion (Tao et al., 2004). Using transgenic mice with cardiac-specific overexpression of Trx1 (Tg-Trx1) or its dominant-negative form (Tg-DN-Trx1), we have demonstrated previously that one of the prominent effects of Trx1 in the heart is to inhibit hypertrophy (Yamamoto et al., 2003).

Gene expression is controlled in part by the acetylation and deacetylation of histones, the latter of which is mediated by a group of molecules called histone deacetylases (HDACs). Among them, class II HDACs are expressed only in nonproliferative cells, including myocytes (Bucks and Olson, 2006). Dynamic nucleocytoplasmic shuttling has been proposed as one of the most fundamental mechanisms regulating the function of class II HDACs (McKinsey et al., 2000). Phosphorylation of class II HDACs at specific serine residues after hypertrophic stimulation induces the interaction with 14-3-3 that leads to masking of the nuclear localization signal (NLS) from importin α and unmasking of the nuclear export signal (NES) to CRM1 (exportin). The class II HDACs are thereby exported to the cytosol, where they can no longer suppress target transcription factors. In the heart, nuclear export of class II HDACs directly elicits activation of nuclear factor of activated T cell (NFAT) and myocyte enhancer factor 2 (MEF2), master positive regulators of cardiac hypertrophy (Bucks and Olson, 2006). Although class II HDACs may be regulated by other forms of posttranslational modification, such as sumoylation and ubiquitination, as well (Kirsh et al., 2002; Potthoff et al., 2007), a redox-dependent mechanism has not been demonstrated previously.

We here demonstrate that Trx1 regulates the nucleocytoplasmic shuttling of class II HDACs through a redox-dependent mechanism. By forming a multiprotein complex with DnaJb5, a heat shock protein 40, and TBP-2, a Trx1-binding protein, Trx1 reduces HDAC4, a class II HDAC, at Cys-667 and Cys-669, which are easily oxidized to form a disulfide bond in response to hypertrophic stimuli. The redox status of these cysteines critically affects the localization of HDAC4, thereby regulating cardiac hypertrophy. The molecular link between the redox-regulating protein Trx1 and class II HDACs may provide new insight into the mechanism by which redox regulates the development of cardiac hypertrophy.

RESULTS

Trx1 Upregulates DnaJb5 in Mouse Hearts and Cardiac Myocytes

In order to search for genes that are regulated by Trx1 in the heart and suppress cardiac hypertrophy, we performed DNA microarray analyses (Ago et al., 2006). We identified *DnaJb5* as one of the genes specifically upregulated in Tg-Trx1 but not in Tg-DN-Trx1 (Figure S2). Consistently, protein expression of DnaJb5 was upregulated in both Tg-Trx1 mice (Figure 1A) and Trx1-overexpressing myocytes (Figure 1B). Conversely, treatment with short hairpin RNA (shRNA) against Trx1 (shTrx1) decreased the expression of DnaJb5 in myocytes (Figure 1C). Trx1 also upregulated expression of Hsp70, albeit to a lesser extent (Figures 1A–1C). Immunocytochemistry and immunoblot analyses showed that both Trx1 and DnaJb5 are localized in both the nucleus and cytosol in cultured myocytes under serum-free conditions (Figures 1D and 1E), as well as in mouse hearts at baseline (Figure 1E).

DnaJb5 Associates with Trx1 through Interaction with TBP-2 and Enhances the Activity of Trx1

We examined the possibility that Trx1 interacts with DnaJb5. Pull-down assays revealed that although DnaJb5 did not bind

to Trx1 directly (Figure 1F, left), it strongly interacted with TBP-2 (Figure 1F, right). Physical interaction between endogenous DnaJb5 and TBP-2 in cardiac myocytes was confirmed in the presence or absence of a hypertrophic stimulus, such as PE (Figure 1G and Figure S3).

We next examined whether DnaJb5 affects the interaction between Trx1 and TBP-2. Pull-down assays showed that TBP-2 interacts with HA-Trx1 in COS7 cells. When HA-DnaJb5 was overexpressed together with HA-Trx1, it did not interfere with the interaction between Trx1 and TBP-2, suggesting that DnaJb5 can form a complex with Trx1 and TBP-2 (Figure S4). Because TBP-2 was originally reported to be an inhibitor of Trx1 (Nishiyama et al., 1999), we examined whether DnaJb5 affects the reducing activity of Trx1 in the complex. Consistent with the previous report, TBP-2 significantly suppressed the reducing activity of Trx1 when TBP-2 was co-overexpressed with Trx1 in COS7 cells (Figure 1H). However, when DnaJb5 was co-overexpressed together with Trx1 and TBP-2, the reducing activity of Trx1 was significantly restored (Figure 1H).

TBP-2 Mediates Nuclear Localization of Trx1 and DnaJb5

Because TBP-2 interacts with importin α_1 , a component of the nuclear import machinery (Nishinaka et al., 2004), we hypothesized that TBP-2 mediates the nuclear localization of Trx1 and DnaJb5. Immunoblot analyses showed that shRNA against TBP-2 (shTBP-2) significantly decreased Trx1 and DnaJb5 levels in the nucleus and increased them in the cytosol of cardiac myocytes (Figure 1I). These findings suggest that TBP-2 mediates the nuclear localization of Trx1 and DnaJb5.

Trx1 and DnaJb5 Suppress PE-Induced NFAT Activation and Cardiac Hypertrophy

To explain the antihypertrophic effect of Trx1, we hypothesized that Trx1 and DnaJb5 suppress the activity of key transcription factors that lead to cardiac hypertrophy, such as NFAT (Molkentin et al., 1998). Treatment with PE (Figure 2A) or overexpression of catalytically active calcineurin (Figure S5) increased the activity of NFAT, as determined by reporter gene assays in myocytes. Overexpression of Trx1, DnaJb5, or TBP-2 significantly suppressed both PE- and calcineurin-induced activation of NFAT (Figure 2A and Figure S5). The suppressive effect of Trx1 on the NFAT activity was completely abolished when either shRNA of DnaJb5 (shDnaJb5) or shTBP-2 was cotransfected with Trx1 (Figure 2A). We also examined the effect of Trx1, DnaJb5, or TBP-2 on expression of *atrial natriuretic factor* (ANF), a target gene of NFAT (Molkentin et al., 1998), and cardiac hypertrophy in response to PE. Trx1, DnaJb5, and TBP-2 suppressed the PE-induced increases in ANF expression, cell size, and protein content, whereas knockdown of either DnaJb5 or TBP-2 attenuated the Trx1-mediated suppression of these parameters (Figures 2B and 2C). These findings suggest that overexpression of either Trx1, DnaJb5 or TBP-2 suppresses PE-induced cardiac hypertrophy and that both DnaJb5 and TBP-2 are required for Trx1-induced suppression of cardiac hypertrophy.

To confirm the suppressive effect of Trx1 on NFAT activity in vivo, we made bitransgenic mice harboring both a *Trx1* transgene and NFAT-reporter gene. Infusion of PE into NFAT-reporter

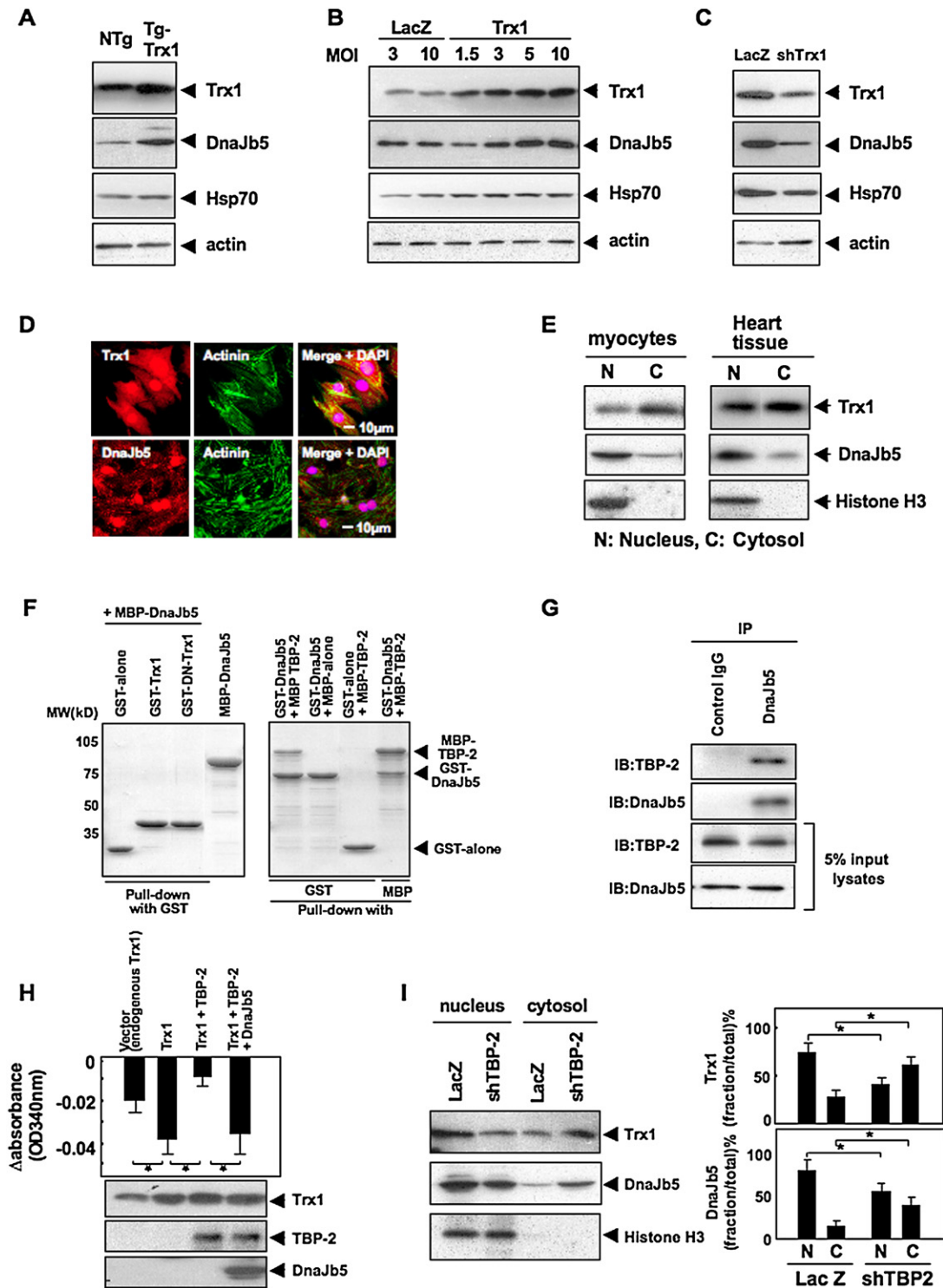


Figure 1. Trx1 Upregulates DnaJb5 and Forms a Complex with DnaJb5 via TBP-2

(A–C) Expression of Trx1, DnaJb5, Hsp70, and actin was examined by immunoblot, through the use of NTg and Tg-Trx1 heart homogenates (A) or myocytes transduced with the indicated adenovirus (B and C).

(D) Myocytes cultured under serum-free conditions were stained with a Trx1 or DnaJb5 antibody (red), an actinin antibody (green), and DAPI (blue).

(E) Expression of Trx1 and DnaJb5 was examined by immunoblot, through the use of cytosolic and nuclear fractions of cultured myocytes or mouse hearts.

(F) Interaction between Trx1 and DnaJb5 (left) or between TBP-2 and DnaJb5 (right) was examined by pull-down assays with the indicated recombinant proteins.

mice without Trx1 overexpression increased the activity of NFAT in the heart and induced cardiac hypertrophy (Figure 2D), both of which were attenuated in Trx1 overexpression mice (Figure 2D). These findings indicate that Trx1 suppresses PE-induced NFAT activation and cardiac hypertrophy *in vivo* as well as *in vitro*.

DnaJb5 Directly Binds to the HDAC Domain of Class II HDACs

Class II HDACs inhibit the activity of key transcription factors mediating cardiac hypertrophy, such as NFAT and MEF2 (Bucks and Olson, 2006). A variant form of Mrj (DnaJb6), another DnaJ family protein, interacts with HDAC4 (Dai et al., 2005). We therefore hypothesized that DnaJb5 upregulated by Trx1 recruits class II HDACs into the nucleus and suppresses cardiac hypertrophy.

Coimmunoprecipitation assays showed that DnaJb5 interacts physically with HDAC4 in myocytes (Figure 3A). The primary structure of the HDAC domain is conserved among all class II HDACs. The HDAC domain of HDAC4 alone was sufficient for interaction with DnaJb5, whereas even full-length HDAC4 did not interact with DnaJb1, another DnaJ protein (Figure 3B). In addition, the HDAC domain of HDAC5, another class II HDAC, also interacted with DnaJb5 (Figure S6). Truncated mutants of the HDAC domain, HDAC4 (628–971) and HDAC4 (628–881), were able to interact with DnaJb5 (Figure 3C). However, our attempt at making the further truncated HDAC4 (628–768) resulted in an insoluble protein, leaving HDAC4 (628–881) as the minimum DnaJb5 interaction domain identified. A HDAC4 mutant in which residues 628–881 are deleted (HDAC4 Δ 628–881) failed to interact with DnaJb5 (Figure 3D). Interestingly, HDAC4 Δ 628–881 was localized in the cytosol (Figure 3D). These findings suggest that a part of the HDAC domain (628–881) is necessary for the HDAC4–DnaJb5 interaction and determines the subcellular localization of HDAC4. As for DnaJb5, pull-down assays showed that the C-terminal region of DnaJb5 (residues 71–348) is necessary and sufficient for the interaction with HDAC4 (Figure 3E).

The Redox State of DnaJb5, Regulated by Trx1, Affects Its Interaction with HDAC4 and HDAC4 Localization

To test the possibility that the interaction between DnaJb5 and HDAC4 is regulated by redox, we examined the effect of H₂O₂ on the interaction. Treatment with H₂O₂ did not affect the stability of either DnaJb5 or HDAC4 (Figure 4A). However, the interaction between DnaJb5 and HDAC4 was significantly attenuated by H₂O₂ in a dose-dependent manner (Figure 4A). Thus, we examined whether DnaJb5 is modified by redox, using mass spectrometry (MS) analysis. The MS/MS spectra showed that, under oxidizing conditions, Cys-274 and Cys-276 in DnaJb5 readily form a disulfide bond (Figure 4B1) which was reduced by tris

(2-carboxyethyl) phosphine (TCEP), a reducing reagent (Figure 4B2). To test whether Trx1 reduces these cysteines, we performed a Trx1 reduction assay. The MS showed that Trx1 significantly reduced the oxidized peptide of DnaJb5 (residues 271–286) (Figure 4C2) compared to buffer alone and DN-Trx1 (Figures 4C1 and 4C3).

For further confirmation that Cys-274 and Cys-276 in DnaJb5 are oxidized to form a disulfide bond *in situ*, HA-DnaJb5 immunoprecipitated from myocyte lysates treated with iodoacetamide (IAM), a reagent which covalently binds to the thiol group of reactive cysteines in their reduced forms, was subjected to MS analyses. DnaJb5 exists predominantly as an IAM-labeled reduced form (m/z 1775.84) under serum-free conditions (Figures 4D1, 4D4, and 4D6). In response to PE treatment, a peptide containing a disulfide bond between Cys-274 and Cys-276 (m/z 1659.79) (Figure 4D5) increased significantly, whereas the mass of IAM-labeled peptide was decreased (Figures 4D2 and 4D4). The increased disulfide bond formation reverted to control levels when Trx1 was coexpressed (Figures 4D3 and 4D4). These results suggest that Cys-274 and Cys-276 in DnaJb5 are oxidized in response to hypertrophic stimuli and reduced by Trx1 in cardiac myocytes.

We further examined the role of Cys-274 and Cys-276 in mediating the interaction between DnaJb5 and HDAC4. Treatment of cardiac myocytes with PE attenuated the interaction between both endogenous and overexpressed DnaJb5 and HDAC4 (Figure 4E and Figure S3). The DnaJb5 C274/276S mutant failed to interact with HDAC4 even in the absence of PE (Figure 4E), suggesting that intact cysteines are required for the interaction. The interaction was also attenuated by ethylene diamine tetraacetic acid (EDTA) and enhanced by zinc chloride (Figure 4F), suggesting that Cys-274 and Cys-276 in DnaJb5 participate in zinc coordination and that disruption of the zinc-thiol interaction inhibits the interaction between DnaJb5 and HDAC4. On the other hand, the DnaJb5 C274/276S mutant was able to interact with TBP-2, suggesting that the interaction between DnaJb5 and TBP-2 is not regulated by modification of Cys-274/Cys-276 (Figure S7).

We further examined the effect of the DnaJb5 C274/276S mutant on the localization of HDAC4. When the DnaJb5 C274/276S mutant was overexpressed in myocytes, the nuclear localization of HDAC4 was significantly attenuated (Figure 4G). Consistently, the C274/276S substitution abolished the suppressive effect of DnaJb5 on NFAT activity in myocytes stimulated with PE (Figure 4H).

Trx1 Suppresses Nuclear Export of HDAC4 Induced by PE

Because HDAC4 has multiple cysteine residues in its HDAC domain, we tested the possibility that Trx1 reduces HDAC4 and

(G) Coimmunoprecipitation assays with myocyte lysates. After immunoprecipitation with control IgG or a DnaJb5 antibody, immunoblots for endogenous DnaJb5 and TBP-2 were performed. Immunoblots of input controls (5% lysates) are also shown.

(H) Through the use of lysates of COS7 cells transfected with the indicated vectors, Trx-reducing activity was examined. Expression of the indicated proteins was examined by immunoblot and analyzed densitometrically. Error bars indicate standard errors (n = 6, *p < 0.05).

(I) Effects of shTBP-2 on the localization of Trx1 and DnaJb5 were examined by immunoblot. Seventy-two hours after treatment with either LacZ or shTBP-2, the cytosolic and nuclear fractions were prepared from myocytes. The percentage of total Trx1 or DnaJb5 in each compartment was obtained by densitometric analyses. Error bars indicate standard errors (n = 4, *p < 0.05).

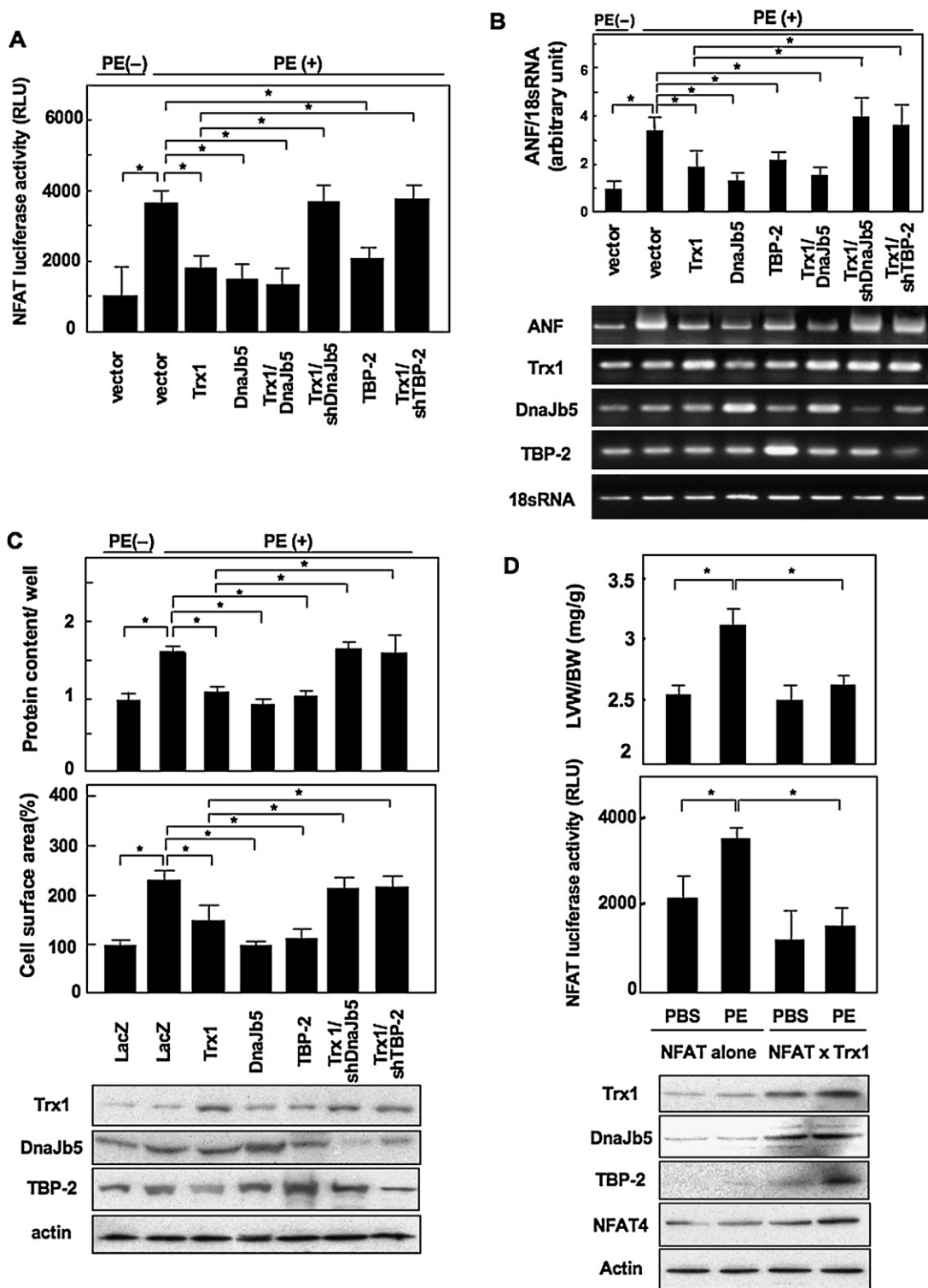


Figure 2. Trx1 and DnaJb5 Inhibit PE-Induced NFAT Activation and Cardiac Hypertrophy

(A) Myocytes were transfected with the indicated vectors and an NFAT-luciferase reporter vector (n = 15, *p < 0.05). Error bars indicate standard errors. (B) The effects of the indicated adenoviruses on ANF expression were examined by quantitative RT-PCR. ANF expression was normalized by 18S rRNA. Error bars indicate standard errors (n = 5, *p < 0.05). Expression of the indicated molecules was determined by RT-PCR. (C) Relative protein content and cell surface area of myocytes treated with the indicated adenoviruses in the presence or absence of PE for 72 hr were examined. Error bars indicate standard errors (n = 6, *p < 0.05). Expression levels of the indicated proteins were examined by immunoblots.

affects its localization. As reported (Backs and Olson, 2006), HDAC4 was exported from the nucleus to the cytosol in myocytes in response to PE (Figure 5A). However, the nuclear export was drastically suppressed by overexpression of Trx1 but not DN-Trx1 (Figure 5A). Because Trx1 did not affect the PE-induced phosphorylation state of HDAC4, Trx1 may regulate the localization of HDAC4 independently of phosphorylation (Figure 5B).

Identification of Redox-Sensitive Cysteines in HDAC4

We next sought to identify redox-sensitive cysteines in HDAC4 by using MS analysis. We used GST-HDAC domain of HDAC4 (residues 628–1040) because 11 of the 14 cysteines in HDAC4 are located in this region. Among these, nine cysteines were detected in the MS analysis after trypsin or glutamic C endopeptidase (Glu-C) digestion, whereas two cysteines (Cys-700 and Cys-1030) were not because the mass signal of peptides containing these two cysteines was buried in the matrix background. Among the nine cysteines, Cys-667 and Cys-669 (Figure 5C) and Cys-982 and Cys-988 (Figure S8) formed disulfide bonds under oxidizing conditions that were reduced by TCEP, whereas the other five (Cys-698, Cys-751, Cys-777, Cys-813, and Cys-952) were found in a reduced form and were unaffected by up to 250 μ M H₂O₂ treatment. The four redox-modifiable cysteines are conserved in class II HDACs. Importantly, Cys-667 and Cys-669 are located in the loop region, which is not present in other classes of HDAC (Figure 5D). The disulfide bond between Cys-982 and Cys-988 may form only in a digested peptide because, based on the ternary-structured model, Cys-982 and Cys-988 may be too far apart to form a disulfide bond in an α helix stretch (Vannini et al., 2004). MS showed that Trx1 significantly reduced the oxidized peptide of HDAC4 (residues 665–681) (Figure 5E2) compared to buffer alone and DN-Trx1 (Figures 5E1 and 5E3). Consistently, Trx1 failed to reduce the HDAC domain having the C667/669S substitution (Figure S9), supporting the notion that Trx1 specifically reduces Cys-667 and Cys-669 in HDAC4.

Significance of the Redox-Sensitive Cysteines, Cys-667 and Cys-669, in HDAC4

We examined whether HDAC4 is oxidized in myocytes in response to hypertrophic stimulation. The extent of cysteine reduction in HDAC4 was determined with biotinylated IAM. When myocytes were treated with PE, levels of free thiol in HDAC4 were significantly decreased within 5 min (Figure 6A). Reduced cysteines were hardly detected in the HDAC4 C667/669S mutant at baseline. These results suggest that Cys-667 and Cys-669 are major reactive thiols that are rapidly oxidized in response to PE (Figure 6A). Overexpression of Trx1, but not of DN-Trx1, attenuated the PE-induced oxidation of HDAC4 (Figure 6A). Importantly, the time course of oxidation was faster than that of the PE-induced phosphorylation, which occurred gradually after 60 min treatment with PE (Figure 6A). Immunostaining showed that nuclear export of HDAC4 started occurring within 5 min after PE treatment (Figure 6B), suggesting that ox-

idation may initiate nuclear export of HDAC4 independently of phosphorylation.

To elucidate the functional roles of cysteine modification at Cys-667 and Cys-669 in HDAC4, we examined the localization of the HDAC4 C667/669S and C667/669A mutants in myocytes. In contrast to the localization of wild-type HDAC4, both of the HDAC4 mutants were localized exclusively in the cytosol, even without PE treatment (Figure 6C). The nuclear export of the mutants was completely suppressed by 10 nM leptomycin B (LMB), a specific inhibitor of CRM1 (exportin) (Figure 6C), suggesting that the HDAC4 mutants are exported to the cytosol in a CRM1-dependent manner. When wild-type HDAC4 was transfected into myocytes, NFAT activity was significantly suppressed (Figure 6D). Both the C667/669S and the C667/669A mutants significantly enhanced NFAT activity in the absence of PE and failed to inhibit PE-induced increases in NFAT activity (Figure 6D). These results suggest that the intact cysteines are required for the nuclear localization of HDAC4.

To test the effect of the C667/669S substitution on cardiac hypertrophy in vivo, we attempted to generate transgenic mice with cardiac-specific overexpression of wild-type HDAC4 (Tg-HDAC4), as well as the C667/669S mutant (Tg-HDAC4 C667/669S). We established four independent lines of Tg-HDAC4 C667/669S and used two lines, #21 and #40, for further analyses (Figure 6E). In contrast, although we obtained three founders of Tg-HDAC4, the founders either died prematurely or lacked germline transmission. Compared to NTg, Tg-HDAC4 C667/669S displayed significantly greater left ventricular (LV) weight:body weight at 2–3 months of age at baseline (Figure 6E). The cross-sectional area of LV myocytes was significantly greater in Tg-HDAC4 C667/669S than in NTg (Figures 6E and 6F). Consistently, the mRNA level of the cardiac hypertrophy marker gene, *Anf*, was significantly higher in Tg-HDAC4 C667/669S (Figure 6E). The HDAC4 C667/669S mutant was localized primarily in the cytosol in mouse hearts (Figure 6G), suggesting that the HDAC4 C667/669S mutant is exported to the cytosol and disrupts the suppressive effect of HDAC4 on cardiac hypertrophy in vivo.

The HDAC4 C667/669S mutant was able to interact with DnaJb5 to almost the same extent as wild-type HDAC4 in pull-down assays and in immunoprecipitation assays in myocytes (Figures 6H and 6I), suggesting that the HDAC4 C667/669S mutant can act as a dominant negative, possibly through competition with endogenous HDAC4 for association with the DnaJb5-TBP-2-Trx1 complex.

Because the HDAC4 mutant is exported to the cytosol in a CRM1-dependent manner (Figure 6C), we hypothesized that the HDAC domain may physically interact with the NES in a redox-dependent fashion, thereby suppressing exposure of the NES to CRM1. Pull-down assays revealed that the HDAC domain can interact with the NES (residues 1040–1084 in HDAC4) (Figure 6J). Interestingly, the interaction was attenuated by the C667/669S substitution (Figure 6J). The intramolecular interaction was also attenuated by H₂O₂ and EDTA, whereas it was

(D) Mice with the NFAT-reporter gene alone or mice with overexpressed Trx1 and the reporter gene were treated with either PBS or PE (75 mg/kg/day) for 14 days (n = 6 in each group). Cardiac hypertrophy was evaluated by LVW/BW (mg/g) (*p < 0.05). NFAT activity was measured by luciferase activity with heart homogenates (*p < 0.05). Error bars indicate standard errors. Expression levels of the indicated proteins were examined by immunoblots.

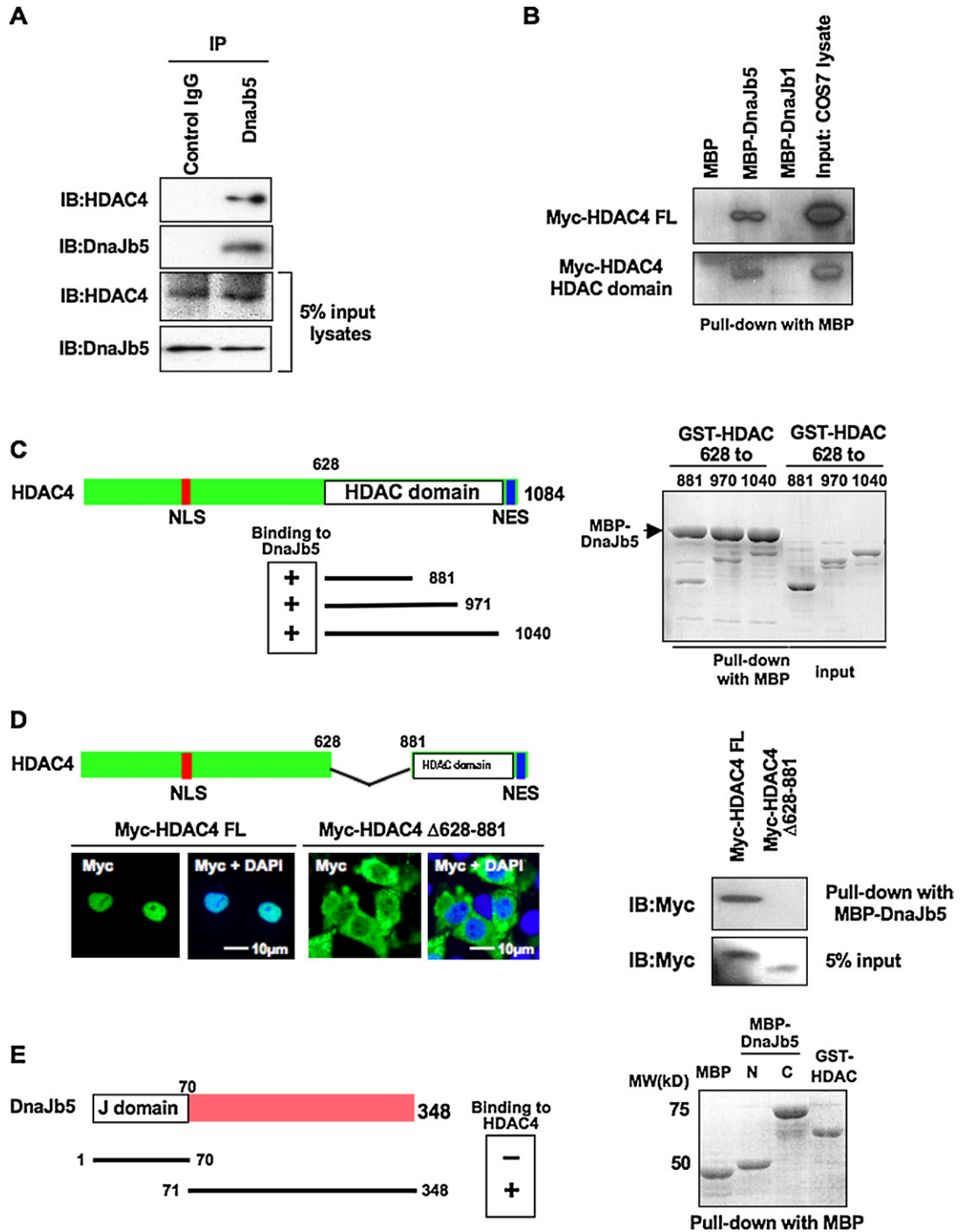


Figure 3. DnaJb5 Interacts with HDAC4

(A) Myocyte lysates were used for immunoprecipitation with either control IgG or a DnaJb5 antibody. Immunoblots for DnaJb5 and HDAC4 were performed. Immunoblots of input controls (5% lysates) are also shown.

(B) Lysates of COS7 cells transfected with myc-HDAC4 full-length (FL) or myc-HDAC domain of HDAC4 (628–1040) were used for pull-down assays with the indicated MBP proteins.

(C) The indicated GST-fused truncated mutants of HDAC4 were incubated with MBP-DnaJb5 for pull-down assays.

(D) Localization of myc-tagged full-length HDAC4 and HDAC4 Δ628-881 was examined in COS7 cells. Cells were stained with a myc antibody (green) and DAPI (blue) (left). Lysates of COS7 cells transfected with the indicated vectors were used for pull-down assays with MBP-DnaJb5. Expression of the myc-proteins was examined by immunoblot (right).

(E) The indicated MBP proteins were incubated with GST-HDAC domain for pull-down assays.

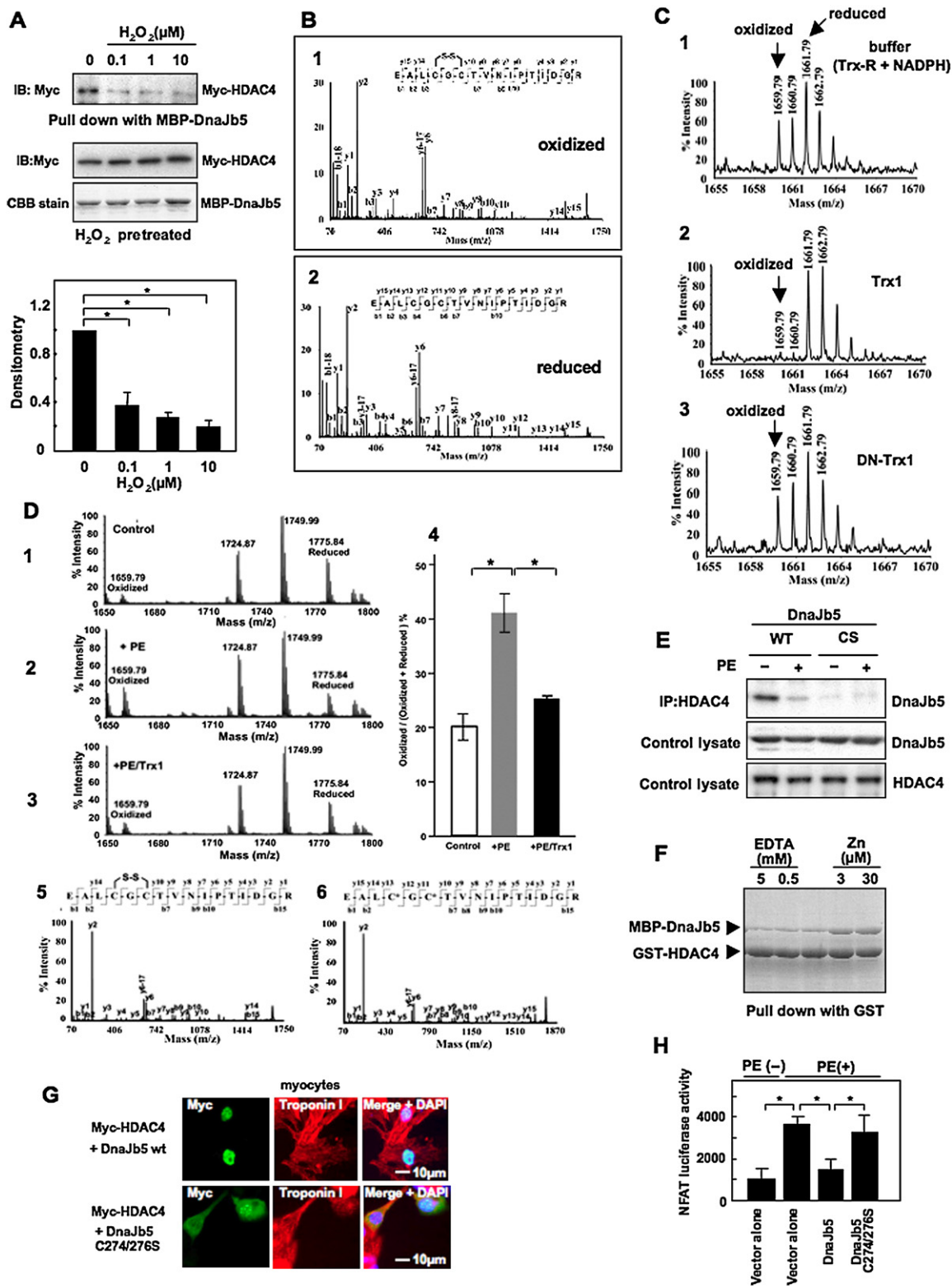


Figure 4. Redox-Regulated Interaction between DnaJb5 and HDAC4

(A) COS7 lysates with HDAC4 overexpression and MBP-DnaJb5 were treated with the indicated concentrations of H₂O₂ for 30 min and subjected to pull-down assays. Statistical analysis of densitometric measurements is shown. Error bars indicate standard errors (n = 3, *p < 0.05).

enhanced in the presence of zinc (Figure 6J). We speculate that Cys-667 and Cys-669 in HDAC4 are involved in zinc coordination and that the presence of the zinc-thiol structure promotes the interaction between the HDAC domain and the NES. Although the HDAC domain could mask the NES through intramolecular interaction under resting conditions, oxidative modification of the cysteines after hypertrophic stimulation may disrupt this interaction and unmask the NES to CRM1, thereby inducing the nuclear export of HDAC4 (Figure 6K).

Does Redox Override Phosphorylation-Regulated Localization of Class II HDACs?

To test the possibility that redox-mediated regulation of HDAC4 overrides phosphorylation-dependent nuclear export, we made a mutant protein in which the three critical serines (at Ser-246, Ser-467, and Ser-632) phosphorylated in response to hypertrophic stimulation were substituted with alanines (3SA), as well as a mutant having both the 3SA and C667/669S substitutions (3SA/C667/669S). Although the 3SA mutant was localized in the nucleus in the resting state, it was exported to the cytosol to some extent in response to PE (Figure 7A). In contrast, the 3SA/C667/669S mutant was localized in the cytosol, even in the absence of hypertrophic stimuli (Figure 7A), indicating that redox modification of HDAC4 at Cys-667 and Cys-669 can direct nuclear export of HDAC4 even in the absence of phosphorylation. The suppression of NFAT activity by the 3SA mutant was also abolished by the addition of the C667/669S substitution (Figure 7B). Consistently, the cell size of myocytes overexpressing the 3SA/C667/669S mutant was significantly greater than that of those overexpressing the 3SA mutant (Figure 7C). To confirm these effects *in vivo*, we transduced adenoviruses harboring the HDAC4 mutants into rat hearts. HDAC4 3SA/C667/669S was localized mainly in the cytosol, in contrast with 3SA, which was localized primarily in the nucleus (Figure 7D). In addition, we injected plasmids harboring either HDAC4 3SA or 3SA/C667/669S together with an ANF-luciferase vector directly into rat hearts. ANF-luciferase activity was greater in rat hearts injected with 3SA/C667/669S than in those with 3SA or vector alone (Figure 7E), supporting the notion that the redox-modification can induce nuclear export of HDAC4 even in the absence of phosphorylation-mediated mechanisms *in vivo*.

We also made a mutant in which the three serines were substituted with aspartates (3SD), a phosphorylation-mimicking

form, and examined its localization and activity. The 3SD mutant was localized in the cytosol and enhanced the activity of NFAT without treatment with PE (Figures 7A and 7B). However, coexpression of Trx1 attenuated the effect of 3SD on nuclear export of HDAC4 and NFAT activation (Figures 7A and 7B). Taken together, these results suggest that redox modification of HDAC4 by Trx1 may be an independent mechanism determining the localization of HDAC4, and it could potentially override the phosphorylation-regulated mechanisms.

DISCUSSION

We demonstrate that Trx1 regulates disulfide bond formation between two cysteine residues located in the HDAC domain of class II HDACs through formation of a multiprotein complex including class II HDACs and DnaJb5. The cysteine residues of HDAC4 are oxidized by hypertrophic stimuli, and mutation of these cysteines was sufficient to induce cardiac hypertrophy *in vivo*. These results suggest that redox regulation of cysteines by Trx1 is a powerful posttranslational mechanism regulating subcellular localization of class II HDACs and cardiac muscle growth.

DnaJb5 Links Trx1 and Class II HDACs, Both Constitutive Negative Regulators of Cardiac Hypertrophy

Our results suggest that DnaJb5 serves to connect Trx1 and class II HDACs, important negative regulators of cardiac hypertrophy (Backs and Olson, 2006; Yamamoto et al., 2003). DnaJ family proteins interact with Hsp70 and function as cochaperones for the ATPase activity of Hsp70 (Qiu et al., 2006). DnaJ proteins play a crucial role in recognizing specific targets, recruiting them to Hsp70, and translocating folded proteins to the proper intracellular organelle, such as the nucleus and mitochondria (Qiu et al., 2006). We speculate that DnaJb5 mediates correct folding and nuclear localization of HDAC4 in the heart.

Is DnaJb5 a Redox-Regulated Chaperone?

A shorter variant of Mrj (DnaJb6) interacts with HDAC4 (Dai et al., 2005). Importantly, however, the shorter form of Mrj contains no cysteines. In contrast, DnaJb5 contains two critical cysteines in its C-terminal region that regulate redox-dependent interaction with HDAC4. Redox-dependent changes in chaperone activity

(B) The MS/MS spectrum of a peptide [271–286] from recombinant GST-DnaJb5 treated with trypsin *in vitro*. The peptide under nonreducing conditions (m/z 1659.79) contained a disulfide bond between Cys-274 and Cys-276 (1). Reduction of the peptide by TCEP produced a mass of 1661.79 due to reduction of the two cysteines (2).

(C) MS spectra of DnaJb5 peptide [271–286] incubated with either the reaction buffer alone (1), Trx1 (2), or DN-Trx1 (3). Trx1 decreased the oxidized peptide (m/z 1659.79) and increased the reduced peptide (m/z 1661.79) (2), compared to buffer alone (1) and DN-Trx1 (3).

(D) Myocytes transduced with HA-tagged DnaJb5 were treated with 100 μ M PE for 4 hr in the presence or absence of Trx1 overexpression. Lysates were prepared in the presence of 200 μ M IAM. HA antibody immunoprecipitates were used for MS analyses. MS at baseline (1), after PE treatment (2), and after PE treatment in the presence of Trx1 (3) are shown. A ratio of the peak height of the oxidized peptide (m/z 1659.79) to the total peptide including both the oxidized and IAM-labeled reduced peptide (m/z 1775.84) is shown (4). MS/MS confirms that the m/z 1659.79 peptide includes a disulfide bond between Cys-274 and Cys-276 (5), and the m/z 1775.84 peptide includes IAM-alkylated cysteines (6).

(E) Effects of PE treatment on the interaction between wild-type DnaJb5 (WT) and HDAC4 or between DnaJb5 CS mutant (CS) and HDAC4 were examined in myocytes overexpressing HDAC4 and DnaJb5 by immunoprecipitation assays. Immunoblots of control lysates are also shown.

(F) Effects of zinc and EDTA on the interaction between DnaJb5 and HDAC4 were examined by pull-down assays.

(G) Effects of overexpression of wild-type DnaJb5 or the C274/276S mutant on the localization of HDAC4. Myocytes were stained with a myc antibody (green), a troponin I antibody (red), and DAPI (blue).

(H) Effects of the DnaJb5 C274/276S mutant on NFAT activity were examined in myocytes. Error bars indicate standard errors ($n = 9$, * $p < 0.05$).

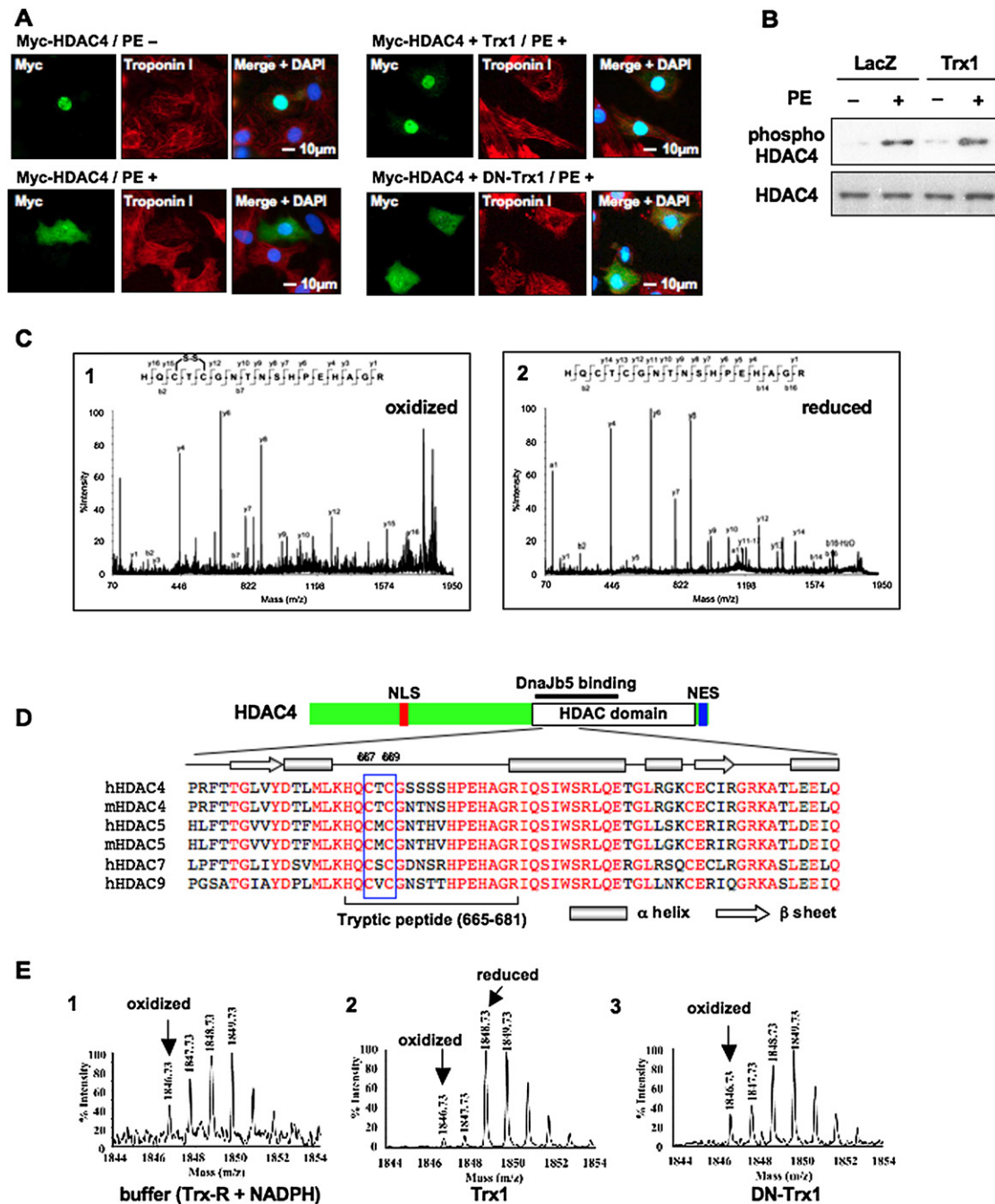


Figure 5. Trx1 Reduces Cysteine Residues at 667 and 669 in HDAC4

(A) The indicated vectors were transfected into myocytes. After treatment with PE (100 µM) or vehicle for 4 hr, myocytes were stained with a myc antibody (green), a troponin I antibody (red), and DAPI (blue).

(B) Myocytes were transfected with HDAC4 and either LacZ or Trx1 adenoviruses. Four hours after treatment with 100 µM PE or vehicle, expression and phosphorylation (at Ser-632) of HDAC4 were examined.

(C) The MS/MS spectrum of a tryptic peptide of HDAC4 [665–681]. The peptide under nonreducing conditions (m/z 1846.73) contained a disulfide bond between Cys-667 and Cys-669 (1). Reduction of the peptide by TCEP produced a peptide mass of 1848.73 in which the two cysteines were reduced (2).

(D) Alignment of HDAC domains (amino acids 650–712 in HDAC4) among class II HDACs is shown. Red-colored amino acids are conserved. The positions of conserved cysteine residues corresponding to Cys-667 and Cys-669 in HDAC4 are indicated by a blue rectangle. Predicted secondary structure is shown above the alignment.

(E) MS spectra of HDAC4 peptide [665–681] incubated with either the reaction buffer alone (1), Trx1 (2) or DN-Trx1 (3). Trx1 decreased the oxidized peptide (m/z 1846.73) and increased the reduced peptide (m/z 1848.73) (2), compared to buffer alone (1) and DN-Trx1(3).

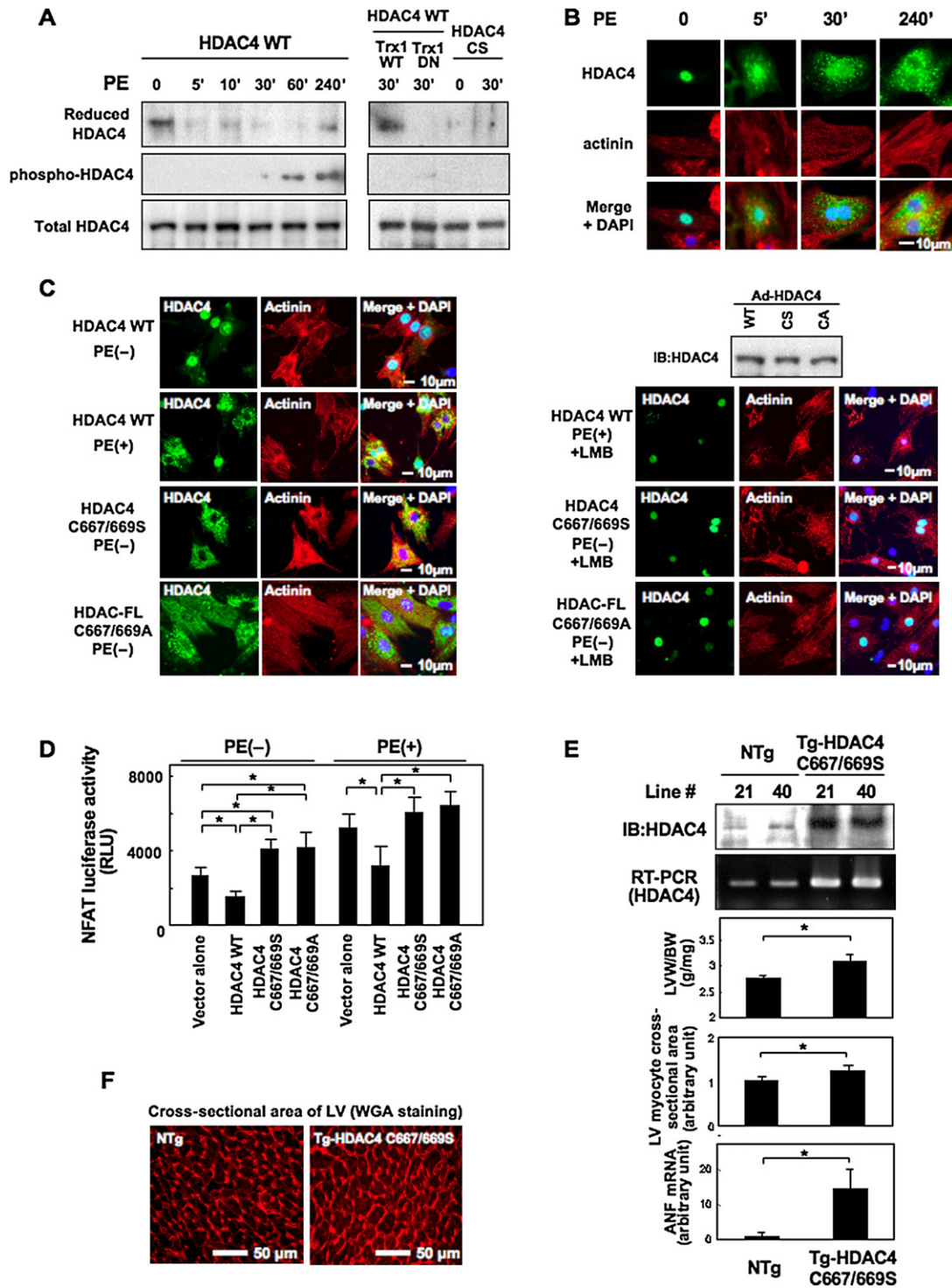
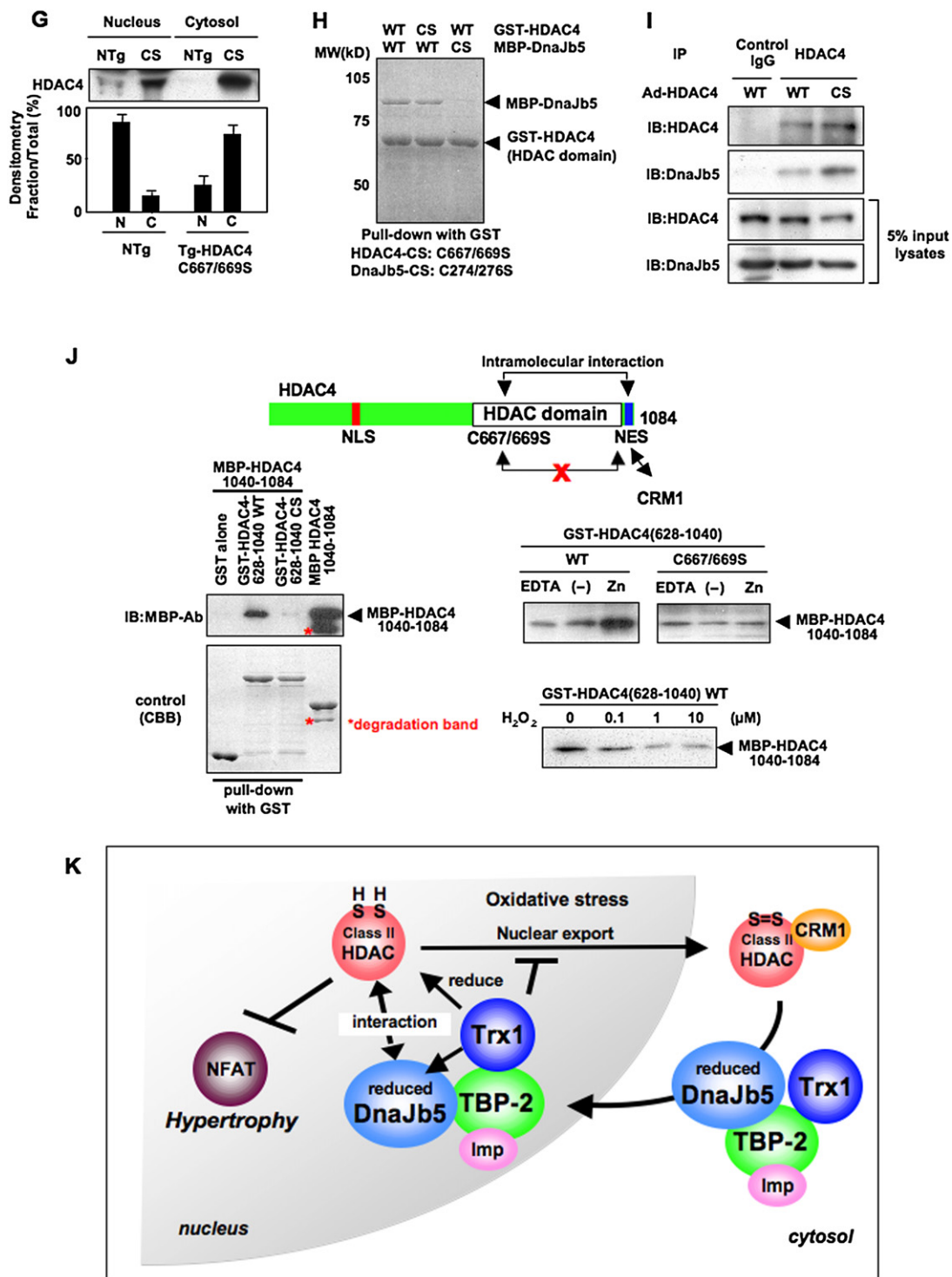


Figure 6. Significance of Cysteines at 667 and 669 in HDAC4

(A) Myocytes transduced with the indicated adenoviruses were treated with PE for the indicated time periods. The extent of reduced cysteines in HDAC4 was detected. Expression and phosphorylation of HDAC4 was examined by immunoblot.
 (B) Time-dependent nuclear export of HDAC4 after PE treatment is shown. Cells were stained with an HDAC4 antibody (green), an actinin antibody (red), and DAPI (blue).
 (C) After transduction with the indicated adenoviruses, myocytes were treated with 100 μM PE for 4 hr with or without 10 nM leptomycin B (LMB). Cells were stained with an HDAC4 antibody (green), an actinin antibody (red), and DAPI (blue). Protein expression of the mutants is also shown.



(D) The effect of the C667/669S or C667/669A substitution on NFAT activity was examined by an NFAT-reporter gene assay in the presence or absence of PE. Error bars indicate standard errors (n = 12, *p < 0.05).

(E) Expression of HDAC4 protein and mRNA in NTg and Tg-HDAC4 C667/669S is shown. Heart size was determined as LVW/BW at 2–3 months of age (n = 10, *p < 0.05). Average cross-sectional area of LV in NTg and Tg-HDAC4 C667/669S is shown (n = 5, *p < 0.05). mRNA level of ANF in NTg and Tg-HDAC4 C667/669S was determined by qPCR (n = 10, *p < 0.05). Error bars indicate standard errors.

(F) Representative WGA staining of NTg and Tg-HDAC4 C667/669S.

(Continued on next page)

have been shown in other DnaJ proteins as well. DnaJa1 contains zinc finger motifs (Cys-x-x-Cys), which coordinate zinc and participate in protein-protein interaction (Choi et al., 2006). DnaJa1 interacts with Trx1, which, in turn, reduces the cysteine residues in the zinc fingers, thereby preserving its chaperone activity (Choi et al., 2006). Although the two reactive cysteines in DnaJb5 do not constitute a typical zinc finger motif, they may participate in zinc coordination because the interaction between DnaJb5 and HDAC4 is enhanced by zinc but attenuated by EDTA. Oxidation or the C274/276S substitution in DnaJb5 may attenuate zinc coordination, thereby suppressing the interaction with HDAC4.

Furthermore, a close relationship between Trx1 and DnaJ proteins has been reported. DnaJb4 interacts with TBP-2 in a yeast two-hybrid system (Nishinaka et al., 2004). Some group C DnaJs contain domains resembling Trx1 (Qiu et al., 2006). Surprisingly, *E. coli* DnaJ itself harbors Trx-like reductase activity (Tang and Wang, 2001). Thus, some, if not all, DnaJ members have redox-regulated functions. Trx1 may regulate the interaction between DnaJb5 and HDAC4, possibly through redox modification of DnaJb5, whereas DnaJb5 maintains the reductase activity of Trx1 despite the presence of TBP-2, suggesting that Trx1 and DnaJb5 assist one another in performing their respective functions.

How Do Trx1 and DnaJb5 Contribute to the Nuclear Localization of HDAC4?

The nuclear localization of HDAC4 is regulated by previously unrecognized mechanisms involving posttranslational oxidative modification of cysteine residues in DnaJb5 and HDAC4. First, the redox state of DnaJb5 may affect the nuclear localization of HDAC4 through direct interaction with HDAC4 because overexpression of the DnaJb5 C274/276S mutant, which cannot interact with HDAC4, attenuates the nuclear localization of HDAC4.

Second, the redox state of HDAC4 itself also affects its localization. In the nonoxidizing state, the HDAC domain may associate with the NES via an intramolecular interaction and block exposure of the NES to CRM1, thereby suppressing the nuclear export of HDAC4. After oxidative modification of Cys-667 and Cys-669, the HDAC domain may dissociate from the NES, which is then exposed to CRM1, thereby inducing the nuclear export of HDAC4. Trx1 may strengthen the interaction between the HDAC domain and the NES, thereby preventing the nuclear export of HDAC4. Because the ultrastructure of the HDAC4 C-terminal end has not been solved, this model awaits confirmation by crystallographic analyses. Importantly, DnaJb5 likely plays an impor-

tant role in bringing Trx1 and HDAC4 into close proximity, so that Trx1 is able to reduce HDAC4 efficiently.

Molecular Structure and Activity of HDAC4

The redox states of Cys-667 and Cys-669 in the HDAC domain are not involved in the interaction with DnaJb5 but play an important role in regulating the localization of HDAC4. This implies a scenario in which oxidized HDAC4 is recognized by DnaJb5, reduced by Trx1 which associates with DnaJb5, and reimported into the nucleus (Figure 6K).

On the other hand, Cys-813, located in the catalytic core, is not oxidized even after treatment with a high concentration of H₂O₂. In addition, the C667/669S substitution did not significantly affect the catalytic activity of HDAC4, at least as measured by transcriptional repression of GAL4-luciferase activity (Figure S10). Thus, the redox regulation may not affect the catalytic activity of HDAC4.

Significance of the Substitution of Redox-Sensitive Cysteine to Serine in DnaJb5 and HDAC4

In general, substitution of a redox-sensitive cysteine to serine in a protein mimics its reduced form because serine is structurally similar to the reduced form of cysteine and it can no longer be oxidized. However, the serine substitution could abolish the function of the molecule when cysteines are catalytically important or mediate coordination of metal, such as zinc, thereby acting similarly to the oxidized form. We speculate that the Cys-to-Ser mutants in DnaJb5 and HDAC4 functionally mimic their oxidized forms, because both the Cys-to-Ser mutations and disulfide bond formation would disrupt the zinc coordination and interaction with HDAC4 and NES, respectively.

Redox- versus Phosphorylation-Mediated Regulation of Class II HDACs

Hypertrophic stimuli induce phosphorylation of serine residues in class II HDACs, thereby leading to nuclear export of the HDACs (Bucks and Olson, 2006; McKinsey et al., 2000). We propose here that redox-mediated regulation is another important mechanism determining the subcellular localization of class II HDACs. Hypertrophic stimuli are often accompanied by increased production of ROS, which could cause thiol oxidation of cysteines (Berndt et al., 2007). Thus, oxidation and phosphorylation of HDAC4 can both take place during hypertrophic responses. Because Trx1 did not affect PE-induced phosphorylation of HDAC4, it is unlikely that Trx1 regulates the activity of upstream kinases of class II HDACs. Indeed, Trx1 failed to inhibit

(G) Protein levels of HDAC4 in the nucleus or cytosol in NTg or Tg-HDAC4 C667/669S mouse hearts were determined by immunoblot. The percentage to total HDAC4 protein in each compartment was analyzed by densitometric analyses.

(H) The effect of the C667/669S substitution in HDAC4 on the interaction with DnaJb5 was examined by pull-down assays.

(I) Interaction of DnaJb5 with either wild-type HDAC4 or the C667/669S mutant was examined by coimmunoprecipitation with lysates of myocytes overexpressing either wild-type or mutant HDAC4. Immunoblots of control lysates are also shown.

(J) The indicated GST proteins were incubated with MBP-HDAC4 NES (1040-1084) for pull-down assays (left). Interaction was detected by immunoblot with an anti-MBP antibody. Effects of zinc, EDTA, and H₂O₂ on the interaction between the HDAC domain and the NES were examined by pull-down assays (right).

(K) A scheme for redox regulation of HDAC4 by Trx1. HDAC4 suppresses positive mediators of cardiac hypertrophy, such as NFAT, in the nucleus when in a reduced state. During oxidative stress, HDAC4 is promptly oxidized and exported to the cytosol, where it can no longer suppress positive mediators of hypertrophy. Reduced DnaJb5, upregulated by Trx1, interacts with HDAC4. Trx1 reduces critical cysteines in HDAC4 by forming a multiprotein complex including DnaJb5, TBP-2, and importin α (Imp), thereby returning HDAC4 to the nucleus.

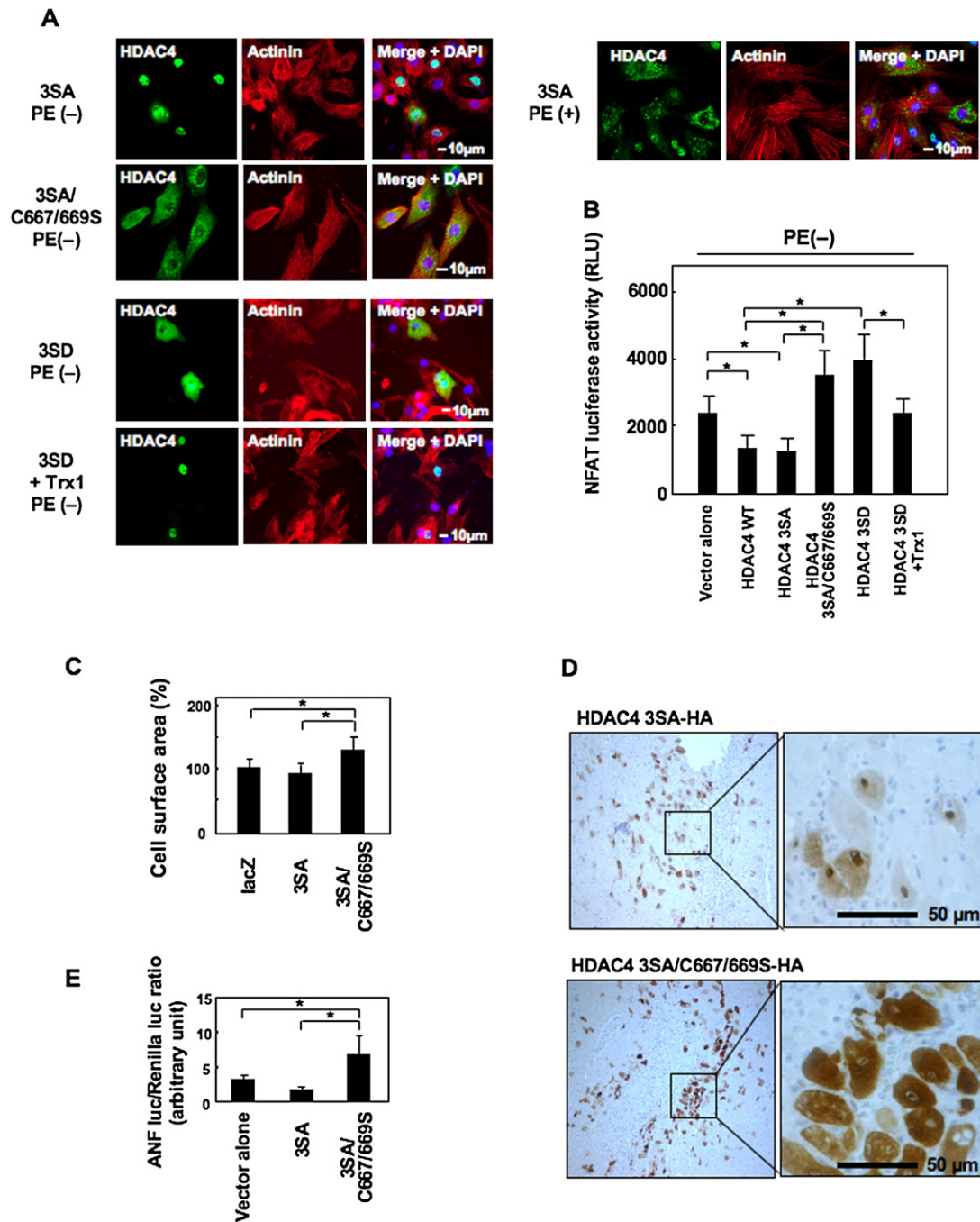


Figure 7. Redox- versus Phosphorylation-Mediated Regulation of Class II HDACs

(A) Myocytes transduced with the indicated adenoviruses were stained with an HDAC4 antibody (green), an actinin antibody (red), and DAPI (blue). As indicated, myocytes were treated with PE for 4 hr.

(B) Effects of the indicated vectors on NFAT activity were determined by NFAT-reporter gene assays in myocytes. Error bars indicate standard errors ($n = 9$, $*p < 0.05$).

(C) Cell surface area was measured in myocytes treated with the indicated adenoviruses. Surface area of myocytes transduced with LacZ was arbitrarily set to 100%. Error bars indicate standard errors ($n = 6$, $*p < 0.05$).

(D) Five days after injection of the indicated HA-tagged adenoviruses, specimens of rat hearts were stained with an HA antibody with the use of a horseradish-peroxidase system.

(E) ANF- and renilla-luciferase vectors and the indicated pcDNA vectors were injected into rat hearts. Five days after injection, heart homogenates were prepared from the injected area, and dual luciferase assays were performed. Error bars indicate standard errors ($n = 4$, $*p < 0.05$).

PE-induced activation of CaMK and PKD (Figure S11), well-known upstream kinases of class II HDACs (Bucks and Olson, 2006). Importantly, oxidation of Cys-667 and Cys-669 and nuclear export of HDAC4 occur more rapidly than phosphorylation after hypertrophic stimulation. These findings suggest that nuclear export of HDAC4 may be biphasic, with redox regulation mediating the early phase of nuclear export. On the other hand, phosphorylation may be needed for a later phase of nuclear export or for maintaining the cytosolic localization of HDAC4 after redox-mediated export. Some of our data also suggest that redox-mediated regulation could override the phosphorylation-mediated one. Thus, targeting redox regulation of HDAC4 could be an independent modality of treatment for cardiac hypertrophy.

In conclusion, we demonstrate a novel mechanism controlling cardiac muscle growth. Both hypertrophic stimuli and Trx1 affect the redox status of the conserved cysteine residues in class II HDACs, which in turn regulates the nucleocytoplasmic localization of class II HDACs and the activity of hypertrophy master key genes, such as NFAT, in cardiac myocytes.

EXPERIMENTAL PROCEDURES

Transgenic Mice

All of the transgenic mice used in this study were generated on an FVB background with the α myosin heavy chain promoter. All protocols concerning animal use were approved by the Institutional Animal Care and Use Committee at the University of Medicine and Dentistry of New Jersey.

Recombinant Proteins and Pull-Down Binding Assays

Proteins fused to glutathione S-transferase (GST) or to maltose binding protein (MBP) were expressed in *E. coli* strain BL21 (DE3) and purified with glutathione Sepharose 4B (Amersham Biosciences) or amylose resin (New England Biolabs).

Immunoblot Analyses

Heart homogenates and cardiac myocyte lysates were prepared in RIPA lysis buffer containing 50 mM Tris (pH 7.5), 150 mM NaCl, 1% IGEPAL CA-630, 0.1% SDS, 0.5% deoxycholic acid, 10 mM $\text{Na}_4\text{P}_2\text{O}_7$, 5 mM EDTA, 0.1 mM Na_3VO_4 , 1 mM NaF, 0.5 mM 4-(2-Aminoethyl) benzenesulfonyl fluoride hydrochloride (AEBSF), 0.5 $\mu\text{g}/\text{ml}$ aprotinin, and 0.5 $\mu\text{g}/\text{ml}$ leupeptin. The nuclear and cytosolic fractions from myocytes and mouse hearts were prepared with NE-PER Nuclear and Cytoplasmic Extraction Reagents (PIERCE).

Immunoprecipitation

Antibodies used for immunoprecipitation (IP) were immobilized to protein A agarose (Santa Cruz) with 50 mM dimethyl pimelimidate (PIERCE) before use. After lysis of myocytes with the RIPA buffer, lysates were incubated with the antibody-immobilized to protein A agarose for 1 hr. After IP products were washed with RIPA buffer three times, they were eluted with 2 \times sample buffer.

Luciferase Assay

Transfection of plasmids into myocytes was performed with Fugene 6 (Roche). Luciferase activity was measured with a luciferase assay system (Promega). The method of in vivo reporter gene assays has been described (Morisco et al., 2001). In brief, 20 μg ANF- and 1 μg renilla-luciferase vectors together with the indicated vectors (1 μg) suspended in 150 μl 0.9% saline were injected into the LV wall. Five days after injection, homogenates were prepared from the injected area with Reporter Lysis Buffer (Promega).

Trx1 Reduction Assay

The activity of Trx1 was detected as a reduction in absorbance at 340 nm, indicating oxidation of NADPH as previously described (Yamamoto et al., 2003). We used recombinant Trx1 or cell lysates.

Mass Spectrometry

Purified GST-DnaJb5 and GST-HDAC domain of HDAC4 were treated with tris (2-carboxyethyl)phosphine (TCEP) or 250 μM H_2O_2 for 10 min at room temperature. For cell samples, lysates of myocytes overexpressing HA-DnaJb5 were subjected to IP with α sarcomeric actin (Sigma). Supernatants were further subjected to IP with HA-agarose (Sigma), and eluates were separated by SDS-PAGE. After staining with coomassie brilliant blue (CBB), HA-DnaJb5 was extracted from the gel. The samples were digested with trypsin or Glu-C and desalted with C_{18} ZipTip (Millipore Corporation) and analyzed on a 4700 Proteomics Analyzer tandem mass spectrometer (Applied Biosystems [ABI]). Positive ion mass spectra were acquired in the reflectron mode. Tandem mass spectra of selected ions were acquired with a method optimized with 1 KV collision energy. Data analysis was performed with Data Explorer software (ABI).

Detection of Thiolate Cysteines

Myocytes transduced with DnaJb5 or HDAC4 adenoviruses were treated with PE in the presence or absence of Trx1 overexpression for the indicated time periods and lysed with lysis buffer containing 200 μM biotinylated-IAM (Molecular Imaging Product Company). Biotinylated proteins were pulled down on streptavidin beads (PIERCE).

Statistical Analysis

All values are expressed as mean \pm SEM. Statistical analyses between groups were done by unpaired Student's *t* test or one-way ANOVA followed by a post hoc Fisher's comparison test. A value of $p < 0.05$ was accepted as significant.

SUPPLEMENTAL DATA

Supplemental Data include Supplemental Experimental Procedures, eleven figures, and Supplemental References and can be found with this article online at <http://www.cell.com/cgi/content/full/133/6/978/DC1/>.

ACKNOWLEDGMENTS

The authors thank Daniela Zablocki for critical reading of the manuscript. This work was supported in part by U.S. Public Health Service Grants HL 59139, HL67727, HL69020, AG23039, AG28787, and HL91469 and by American Heart Association grant 0340123N.

Received: October 4, 2007

Revised: February 2, 2008

Accepted: April 11, 2008

Published: June 12, 2008

REFERENCES

- Ago, T., Yeh, I., Yamamoto, M., Schinke-Braun, M., Brown, J.A., Tian, B., and Sadoshima, J. (2006). Thioredoxin1 upregulates mitochondrial proteins related to oxidative phosphorylation and TCA cycle in the heart. *Antioxid. Redox Signal.* 8, 1635–1650.
- Bucks, J., and Olson, E.N. (2006). Control of cardiac growth by histone acetylation/deacetylation. *Circ. Res.* 98, 15–24.
- Berndt, C., Lillig, C.H., and Holmgren, A. (2007). Thiol-based mechanisms of the thioredoxin and glutaredoxin systems: Implications for diseases in the cardiovascular system. *Am. J. Physiol. Heart Circ. Physiol.* 292, H1227–H1236.
- Cave, A.C., Brewer, A.C., Narayanapanicker, A., Ray, R., Grieve, D.J., Walker, S., and Shah, A.M. (2006). NADPH oxidases in cardiovascular health and disease. *Antioxid. Redox Signal.* 8, 691–728.

- Choi, H.I., Lee, S.P., Kim, K.S., Hwang, C.Y., Lee, Y.R., Chae, S.K., Kim, Y.S., Chae, H.Z., and Kwon, K.S. (2006). Redox-regulated cochaperone activity of the human DnaJ homolog Hdj2. *Free Radic. Biol. Med.* *40*, 651–659.
- Dai, Y.S., Xu, J., and Molkenin, J.D. (2005). The DnaJ-related factor Mrj interacts with nuclear factor of activated T cells c3 and mediates transcriptional repression through class II histone deacetylase recruitment. *Mol. Cell. Biol.* *25*, 9936–9948.
- Hirofani, S., Otsu, K., Nishida, K., Higuchi, Y., Morita, T., Nakayama, H., Yamaguchi, O., Mano, T., Matsumura, Y., Ueno, H., et al. (2002). Involvement of nuclear factor-kappaB and apoptosis signal-regulating kinase 1 in G-protein-coupled receptor agonist-induced cardiomyocyte hypertrophy. *Circulation* *105*, 509–515.
- Kirsh, O., Seeler, J.S., Pichler, A., Gast, A., Muller, S., Miska, E., Mathieu, M., Harel-Bellan, A., Kouzarides, T., Melchior, F., and Dejean, A. (2002). The SUMO E3 ligase RanBP2 promotes modification of the HDAC4 deacetylase. *EMBO J.* *21*, 2682–2691.
- Kwon, S.H., Pimentel, D.R., Remondino, A., Sawyer, D.B., and Colucci, W.S. (2003). H₂O₂ regulates cardiac myocyte phenotype via concentration-dependent activation of distinct kinase pathways. *J. Mol. Cell. Cardiol.* *35*, 615–621.
- Li, G., Chen, Y., Saari, J.T., and Kang, Y.J. (1997). Catalase-overexpressing transgenic mouse heart is resistant to ischemia-reperfusion injury. *Am. J. Physiol.* *273*, H1090–H1095.
- McKinsey, T.A., Zhang, C.L., Lu, J., and Olson, E.N. (2000). Signal-dependent nuclear export of a histone deacetylase regulates muscle differentiation. *Nature* *408*, 106–111.
- Molkenin, J.D., Lu, J.R., Antos, C.L., Markham, B., Richardson, J., Robbins, J., Grant, S.R., and Olson, E.N. (1998). A calcineurin-dependent transcriptional pathway for cardiac hypertrophy. *Cell* *93*, 215–228.
- Morisco, C., Zebrowski, D.C., Vatner, D.E., Vatner, S.F., and Sadoshima, J. (2001). Beta-adrenergic cardiac hypertrophy is mediated primarily by the beta(1)-subtype in the rat heart. *J. Mol. Cell. Cardiol.* *33*, 561–573.
- Nakamura, H., Nakamura, K., and Yodoi, J. (1997). Redox regulation of cellular activation. *Annu. Rev. Immunol.* *15*, 351–369.
- Nishinaka, Y., Masutani, H., Oka, S., Matsuo, Y., Yamaguchi, Y., Nishio, K., Ishii, Y., and Yodoi, J. (2004). Importin alpha1 (Rch1) mediates nuclear translocation of thioredoxin-binding protein-2/vitamin D₃-up-regulated protein 1. *J. Biol. Chem.* *279*, 37559–37565.
- Nishiyama, A., Matsui, M., Iwata, S., Hirota, K., Masutani, H., Nakamura, H., Takagi, Y., Sono, H., Gon, Y., and Yodoi, J. (1999). Identification of thioredoxin-binding protein-2/vitamin D₃ up-regulated protein 1 as a negative regulator of thioredoxin function and expression. *J. Biol. Chem.* *274*, 21645–21650.
- Potthoff, M.J., Wu, H., Arnold, M.A., Shelton, J.M., Backs, J., McAnally, J., Richardson, J.A., Bassel-Duby, R., and Olson, E.N. (2007). Histone deacetylase degradation and MEF2 activation promote the formation of slow-twitch myofibers. *J. Clin. Invest.* *117*, 2459–2467.
- Qiu, X.B., Shao, Y.M., Miao, S., and Wang, L. (2006). The diversity of the DnaJ/Hsp40 family, the crucial partners for Hsp70 chaperones. *Cell. Mol. Life Sci.* *63*, 2560–2570.
- Rajasekaran, N.S., Connell, P., Christians, E.S., Yan, L.J., Taylor, R.P., Orosz, A., Zhang, X.Q., Stevenson, T.J., Peshock, R.M., Leopold, J.A., et al. (2007). Human alphaB-crystallin mutation causes oxidoreductive stress and protein aggregation cardiomyopathy in mice. *Cell* *130*, 427–439.
- Siwik, D.A., Tzortzis, J.D., Pimental, D.R., Chang, D.L., Pagano, P.J., Singh, K., Sawyer, D.B., and Colucci, W.S. (1999). Inhibition of copper-zinc superoxide dismutase induces cell growth, hypertrophic phenotype, and apoptosis in neonatal rat cardiac myocytes in vitro. *Circ. Res.* *85*, 147–153.
- Tang, W., and Wang, C.C. (2001). Zinc fingers and thiol-disulfide oxidoreductase activities of chaperone Dna. *J. Biochem. (Tokyo)* *40*, 14985–14994.
- Tao, L., Gao, E., Bryan, N.S., Qu, Y., Liu, H.R., Hu, A., Christopher, T.A., Lopez, B.L., Yodoi, J., Koch, W.J., et al. (2004). Cardioprotective effects of thioredoxin in myocardial ischemia and reperfusion: Role of S-nitrosation. *Proc. Natl. Acad. Sci. USA* *101*, 11471–11476.
- Vannini, A., Volpari, C., Filocamo, G., Casavola, E.C., Brunetti, M., Renzoni, D., Chakravarty, P., Paolini, C., De Francesco, R., Gallinari, P., et al. (2004). Crystal structure of a eukaryotic zinc-dependent histone deacetylase, human HDAC8, complexed with a hydroxamic acid inhibitor. *Proc. Natl. Acad. Sci. USA* *101*, 15064–15069.
- Yamamoto, M., Yang, G., Hong, C., Liu, J., Holle, E., Yu, X., Wagner, T., Vatner, S.F., and Sadoshima, J. (2003). Inhibition of endogenous thioredoxin in the heart increases oxidative stress and cardiac hypertrophy. *J. Clin. Invest.* *112*, 1395–1406.